



HAL
open science

Blue in green: forestation turns blue water green, mitigating heat at the expense of water availability

Olivier Asselin, Martin Leduc, Dominique Paquin, Nathalie de Noblet-Ducoudré, Diana Rechid, Ralf Ludwig

► **To cite this version:**

Olivier Asselin, Martin Leduc, Dominique Paquin, Nathalie de Noblet-Ducoudré, Diana Rechid, et al.. Blue in green: forestation turns blue water green, mitigating heat at the expense of water availability. *Environmental Research Letters*, 2024, 19 (11), pp.114003. 10.1088/1748-9326/ad796c . hal-04720855

HAL Id: hal-04720855

<https://hal.science/hal-04720855v1>

Submitted on 4 Oct 2024

HAL is a multi-disciplinary open access archive for the deposit and dissemination of scientific research documents, whether they are published or not. The documents may come from teaching and research institutions in France or abroad, or from public or private research centers.

L'archive ouverte pluridisciplinaire **HAL**, est destinée au dépôt et à la diffusion de documents scientifiques de niveau recherche, publiés ou non, émanant des établissements d'enseignement et de recherche français ou étrangers, des laboratoires publics ou privés.

LETTER • OPEN ACCESS

Blue in green: forestation turns blue water green, mitigating heat at the expense of water availability

To cite this article: Olivier Asselin *et al* 2024 *Environ. Res. Lett.* **19** 114003

View the [article online](#) for updates and enhancements.

You may also like

- [Biophysical effects on temperature and precipitation due to land cover change](#)
Lucia Perugini, Luca Caporaso, Sergio Marconi et al.
- [Forestation potential in recultivation of disturbed lands for reduction of greenhouse gas emission](#)
E A Kushnir, C O Grigoriyeva, E I Treshchevskaya et al.
- [Assessing climatic benefits from forestation potential in semi-arid lands](#)
Shani Rohatyn, Eyal Rotenberg, Dan Yakir et al.

ENVIRONMENTAL RESEARCH
LETTERS

LETTER






Blue in green: forestation turns blue water green, mitigating heat at the expense of water availability

OPEN ACCESS

RECEIVED
7 June 2024REVISED
27 August 2024ACCEPTED FOR PUBLICATION
6 September 2024PUBLISHED
23 September 2024

Original Content from this work may be used under the terms of the [Creative Commons Attribution 4.0 licence](#).

Any further distribution of this work must maintain attribution to the author(s) and the title of the work, journal citation and DOI.

Olivier Asselin^{1,*} , Martin Leduc¹ , Dominique Paquin¹ , Nathalie de Noblet-Ducoudré², Diana Rechid³  and Ralf Ludwig⁴ ¹ Ouranos, Montréal, Canada² Laboratoire des Sciences du Climat et de l'Environnement, Gif-sur-Yvette, France³ Climate Service Center Germany (GERICS), Helmholtz-Zentrum Hereon, Hamburg, Germany⁴ Ludwig-Maximilians University, Munich, Germany

* Author to whom any correspondence should be addressed.

E-mail: asselin.olivier@ouranos.ca**Keywords:** climate change, land-use changes, forestation, afforestation/reforestation, water cycle, heat waves, surface energy balanceSupplementary material for this article is available [online](#)**Abstract**

In order to meet a stringent carbon budget, shared socioeconomic pathways (SSPs) aligned with the Paris Agreement typically require substantial land-use changes (LUC), such as large-scale forestation and bioenergy crop plantations. What if such a low-emission, intense-LUC scenario actually materialized? This paper quantifies the biophysical effects of LUC under SSP1-2.6 using an ensemble of regional climate simulations over Europe. We find that LUC projected over the 21st century, primarily broadleaf-tree forestation at the expense of grasslands, reduce summertime heat extremes significantly over large swaths of continental Europe. In fact, cooling from LUC trumps warming by greenhouse gas (GHG) emissions, resulting in milder heat extremes by 2100 for about half of the European population. Forestation brings heat relief by shifting the partition of turbulent energy fluxes away from sensible and towards latent heat fluxes. Impacts on the water cycle are then assessed. Forestation enhances precipitation recycling over continental Europe, but not enough to match the boost of evapotranspiration (green water flux). Run-off (blue water flux) is reduced as a consequence. Some regions experience severe drying in response. In other words, forestation turns blue water green, bringing heat relief but compromising water availability in some already-dry regions.

1. Introduction

Given their strong potential for carbon removal, forestation and bioenergy production figure prominently in the shared socioeconomic pathways (SSPs) compliant with the Paris Agreement (Popp 2017, Harper 2018, Roe 2019). Large-scale adoption of these land-based mitigation strategies would involve substantial land-use changes (LUC), altering the surface energy and water fluxes mediated by albedo, evapotranspiration efficiency and roughness (Perugini *et al* 2017, Pongratz *et al* 2021). These biophysical effects are known to influence regional temperature averages (Betts 2000, Lee 2011, Zeng 2017, Huang *et al* 2020) and extremes (Bonan 2001, Lejeune *et al* 2018, Chen and Dirmeyer 2019, Cao

et al 2023), and the partition of water fluxes between evapotranspiration, precipitation and run-off (Bosch and Hewlett 1982, Jackson *et al* 2005, Ellison *et al* 2012, Ellison 2017, Teuling *et al* 2019, Meier *et al* 2021, te Wierik *et al* 2021).

In low-emission scenarios, the relative impacts of LUC on climate and hydrology are expected to be even more important, because the GHG forcing is weak and LUC are particularly intense due to the pressing need for negative emissions (Hirsch 2018, Seneviratne 2018). For instance, SSP1-2.6, the main Paris-aligned scenario adopted by the climate community (O'Neill 2016), projects an expansion of forests and bioenergy crops by an area roughly equivalent to that of Europe over the 21st century (Doelman 2018). This calls for an urgent look

at the potential unintended consequences of LUC implicated by these mitigation strategies, such as albedo-driven warming (Betts 2000, Hasler 2024) or local depletion of water resources (Jackson *et al* 2005, Engel *et al* 2024) by large-scale forestation, but also their possible co-benefits, such as mitigation of heat waves by increasing the fraction of broadleaf species in temperate forests (Schwaab *et al* 2020, Breil *et al* 2023).

In this paper, we quantify the biophysical effects of LUC in Europe under SSP1-2.6. In this ambitious scenario, Europe undergoes large-scale, primarily broadleaf-tree forestation at the expense of grasslands (Doelman 2018). A four-member ensemble of Earth system model (ESM) simulations is dynamically downscaled over Europe using a regional climate model (RCM). For each ESM member, the RCM is run with three different combinations of land covers and GHG concentrations. The effects of LUC and GHG on regional climate and hydrology can thus be isolated. In the following sections, we focus on the biophysical effects of large-scale forestation on summer heat extremes and implications for the water cycle.

2. Methods

2.1. Simulation ensemble

All simulations presented in this paper were produced with the Canadian RCM (CRCM5; Šeparović *et al* 2013, Martynov *et al* 2013) coupled to the Canadian Land Surface Scheme (CLASS; Verseghy 1991, Verseghy *et al* 1993). The model setup used is described in greater detail in the sensitivity study (Asselin *et al* 2022). In this paper, we analyse an ensemble of 12 regional climate simulations (figure 1). These runs are dynamically downscaled global simulations from the Max Planck Institute for Meteorology ESM version 1.2 (MPI-ESM-1.2; Mauritsen 2019). In particular, we used the four first members (rXi1p1f1, X = 1-4) of the lower-resolution ensemble (MPI-ESM-LR-1.2). For each of the four member realisations, we set up three configurations: present GHG and land cover ($G_p L_p$, or control), future GHG but present land cover ($G_f L_p$), and both future GHG and land cover ($G_f L_f$). These three configurations allow us to isolate the respective effects of LUC and GHG on any variable of interest (see appendix A.1 for details).

All runs were performed with a horizontal resolution of 0.11° over the Europe CORDEX domain (<https://cordex.org> (accessed on 30th April 2024)), except that 30 additional grid points were added to the west side of the computational domain so that all land grid cells are free of spurious spatial spin-up effects (Matte *et al* 2017). The analysis presented here excludes a 7 year temporal spin-up, such that climatological means are calculated over 1986–2015 (present GHG) or 2071–2100 (future GHG).

	Present GHG	Future GHG
Present Land Cover	$G_p^X L_p$	$G_f^X L_p$
Future Land Cover		$G_f^X L_f$

Figure 1. Summary of the 12 simulations analysed in this paper. There are three different model configurations: present GHG and land cover (control; $G_p^X L_p$), future GHG but present land cover ($G_f^X L_p$), and future GHG with future land cover ($G_f^X L_f$). The four layers of superimposed tables represent the four members of the MPI-ESM-LR1.2 ensemble (rXi1p1f1, X = 1-4) that were dynamically downscaled for each configuration.

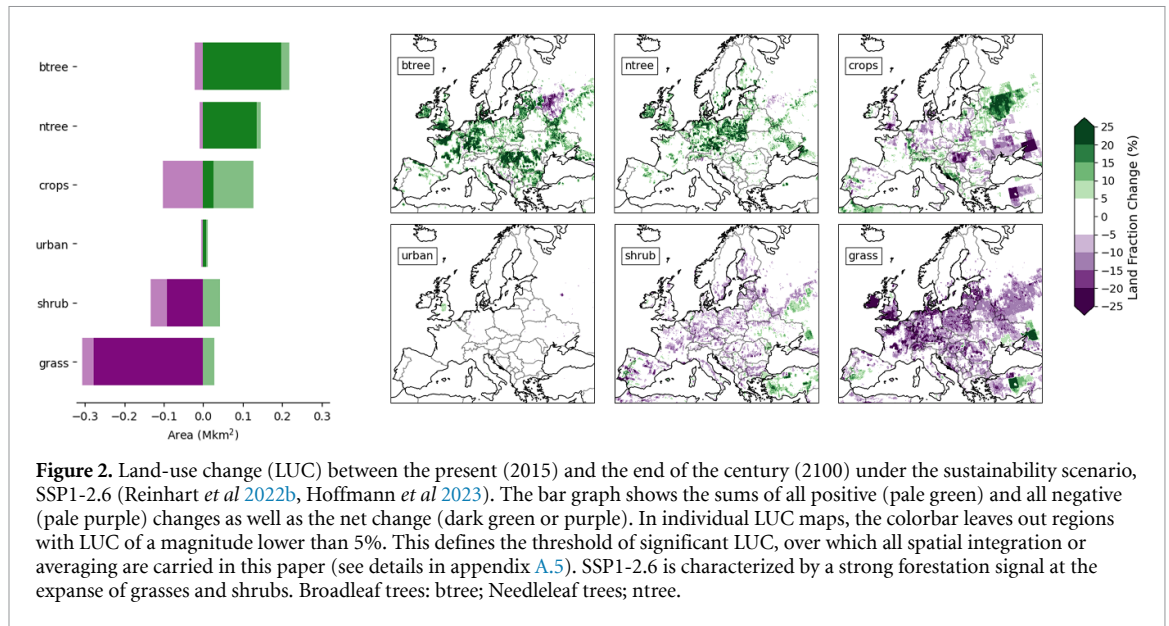
2.2. Future scenario

This paper focuses on the shared socio-economic pathway SSP1-2.6. In this scenario, global population growth levels off by mid-century, diets shift away from animal products, agricultural yields continue to improve and policies are enacted to halt deforestation, promote afforestation and restore degraded forests, resulting in increased forested area and in substantial reductions in grazing land and agricultural land worldwide (Doelman 2018). In Europe, however, the food crop reduction trend is largely canceled by a massive ramp up of biofuel production (Hurtt 2020). In terms of GHG emissions, SSP1-2.6 includes strong mitigation policies limiting global warming to about 2°C above pre-industrial levels by the end of the century (Tebaldi 2020).

2.3. Land cover maps

To quantify the effects of LUC, we need a spatial map of the present land cover as well as the projected changes to that land cover in the future scenario. For the present land cover, we use the version 1.1 of the LANDMATE dataset (Reinhart *et al* 2022a, 2022b), which provides fractions of 16 plant-functional types (PFTs) over Europe for the year 2015. Hoffmann *et al* (2023) developed a land-use translator that generates annual land cover maps based on future projections of land use transitions for different SSPs derived from the Land Use Harmonized Dataset Version 2 (LUH2; Hurtt 2020). In this paper, we use their map for the SSP1-2.6 scenario in year 2100 (Hoffmann *et al* 2022). For consistency with the regional climate simulation ensemble, we chose the 0.1 degree resolution versions of the land cover maps. Note that these maps are publicly available (Hoffmann *et al* 2022, Reinhart *et al* 2022a).

To implement these land cover maps in our model, it is necessary to convert the LANDMATE PFTs to our model's PFTs. The conversion is straightforward as the PFT categories of LANDMATE and CRCM5 are very similar (see table SI-LC1). To simplify the analysis, we aggregate the resulting PFTs into six land cover categories: broadleaf trees (btree), needleleaf trees (ntree), shrubs, grasses, crops, and urban. By construction, the land-use translator does



not change the fraction of bare soil (Hoffmann *et al* 2023). This land category was thus discarded from our analysis.

Figure 2 shows how land cover changes between 2015 to 2100 under SSP1-2.6. Consistent with ambitious carbon sequestration efforts, there is a strong forestation signal in Europe. Broadleaf trees account for most of the increase (about 0.2 Mkm²), followed by needleleaf trees (about 0.14 Mkm²). The land cover type showing the most significant decline is grasses (about -0.28 Mkm²), followed by shrubs (-0.09 Mkm²). There are several regions of strong cropland expansion and reduction, but the net area change is rather weak. Finally, urbanization is comparatively negligible on the continent scale (<0.01 Mkm²) and will therefore be ignored in the rest of our analysis. In terms of land cover change, the SSP1-2.6 may be thought as a more realistic version of the idealized FOREST experiment of the CORDEX Flagship Pilot Study Land-Use and Climate Across Scales (LUCAS) phase 1 (Davin 2020), where all vegetated area were turned into forests. Most of the positive changes in land cover come from forestation, and most of the land replaced is grassland.

3. The green relief: changes in energy fluxes

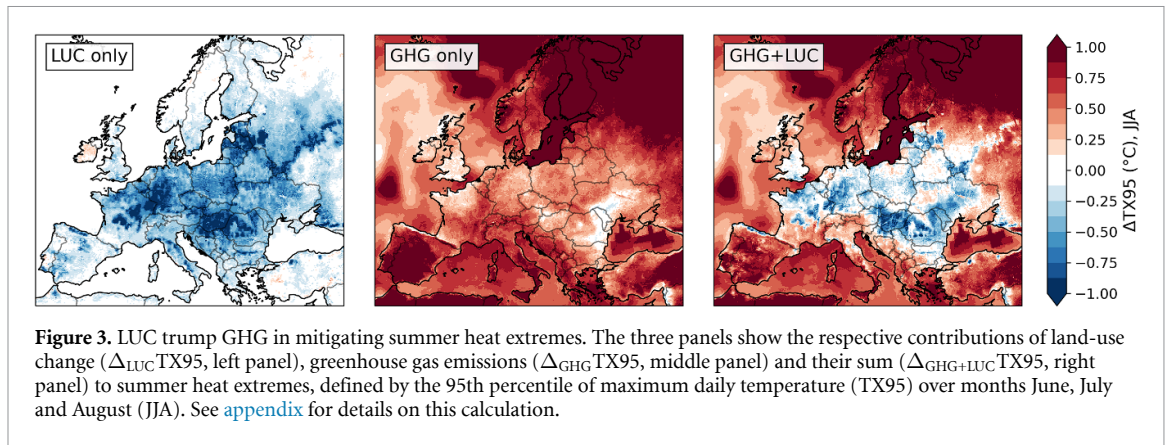
3.1. LUC trump GHG: net mitigation of heat extremes

In this section, we assess the relative contributions of LUC and GHG emissions to end-of-century summertime heat extremes. To do so, we compute the 95th percentile of the maximum daily temperature (TX95) during the summer months (JJA) across the three distinct model configurations of land cover and GHG concentrations in our simulation ensemble (see detailed methodology in appendix).

Figure 3 shows how TX95 is modified by LUC (left panel), GHG (middle panel), and their combined influence (right panel). LUC cause a widespread alleviation of heat extremes over large parts of central and eastern Europe, where most of changes in land-use occur. The heat mitigation pattern is land-confined and distinctly structured. In fact, some of the fine-scale patterns can be recognized from LUC maps—the thin forestation line stretching across southwestern Russia, for instance—hinting that LUC have highly local effects on heat extremes. Of all LUC categories, $\Delta_{\text{LUC}}\text{TX95}$ is best correlated with broadleaf forestation and shrub reduction ($R = -0.57$ and $R = 0.44$, respectively; figure SI-SM1). The cooling effect of LUC is substantial: regions undergoing intense broadleaf forestation respond with a reduction of the TX95 exceeding 1 °C.

GHG emissions, on the other hand, cause a widespread aggravation of heat extremes (middle panel). The GHG response is much smoother and extends to all corners of the domain, including over bodies of water. However, the increase in TX95 is mostly concentrated in the semi-arid Mediterranean region and at high latitudes, leaving a region of modest warming (and even localized mild cooling) in Central Europe. As such, when the effects of both LUC and GHG are combined (right panel), one finds that summertime heat extremes are *reduced* over large swaths of continental Europe. In other words, under SSP1-2.6, LUC (primarily broadleaf forestation) trump GHGs in mitigating summertime heat extremes. Despite GHG-driven global warming, end-of-century heat waves are milder than in the present thanks to forestation.

Using contemporary population data, our estimates suggest that by the end of the century, about half of the European population could experience milder heat waves under this scenario (figure SI-T1;



appendix A.3). In contrast, little more than 1% would benefit from such relief in the absence of forestation efforts. Hence forestation could qualitatively alter the experience of climate change for a significant portion of the European population.

3.2. LUC alter the hot-day surface energy balance

What are the mechanisms by which LUC mitigate heat? To tackle this question, we analyse how LUC modify the surface energy balance. Since we are interested in heat extremes, we focus the analysis on hot days, which we define as summer days with a maximum daily temperature (TX) exceeding its 95th percentile (TX95) for a given configuration (see detailed methodology in [appendix](#)).

Figure 4 shows how LUC alter the surface energy balance during hot summer days. It is clear at first glance that the magnitude of changes in the latent (LH) and sensible heat (SH) fluxes is far greater than changes in shortwave (SW) and longwave (LW) radiation. In other words, LUC predominantly affect turbulent fluxes, with second-order effects on radiative fluxes. Ground heat fluxes (not shown) are dwarfed by both turbulent and radiative fluxes, and are therefore not considered in our analysis.

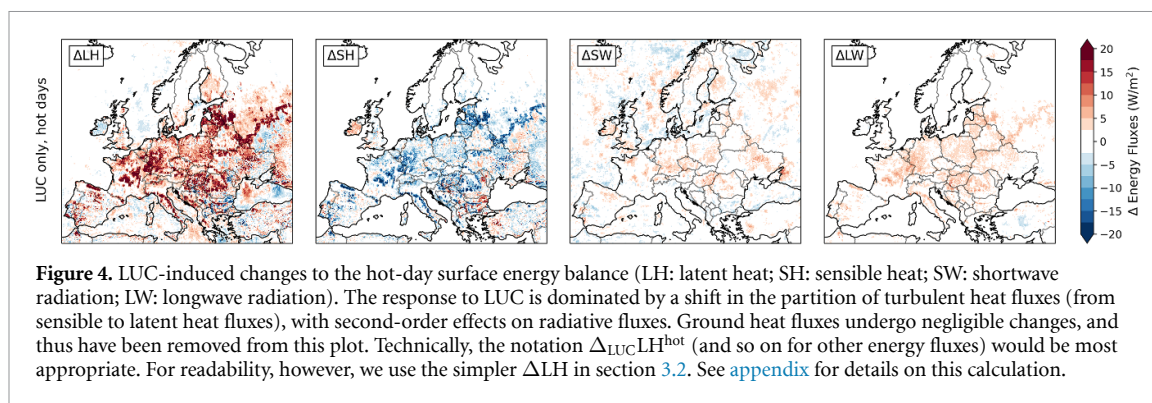
The spatial patterns of LH increase are approximately matched by decreased SH, implying a strong shift in the partition of turbulent fluxes. The fine-scale spatial structure of this shift bears resemblance to the map of heat extreme mitigation due to LUC (figure 3). To quantify this observation, we calculated correlations between LUC-induced, hot-day energy fluxes and maximum daily temperatures (ΔTX ; figure SI-SM2). Patterns of ΔLH match ΔTX very well ($R = -0.76$), with ΔSH following closely behind ($R = 0.65$). This means that on hot days, regions where LUC boost evapotranspiration tend to experience stronger heat relief. In effect, LUC redirects solar energy away from SH, which would otherwise result in warming of the atmosphere. This redirected energy is instead utilized to break hydrogen bonds, i.e. evaporate water, without direct temperature change. The

net result is the well-known phenomenon of evaporative cooling.

Heat extremes match patterns in the longwave signal even better ($R = -0.80$) than latent heat fluxes ($R = -0.76$). This is not surprising as outgoing longwave radiation is slaved to surface temperature. Via Planck's feedback, any change of surface temperature is resisted by the adjustment of upwelling longwave radiation. While the biophysical properties associated with LUC in our model do not directly impact the emission of longwave radiation, LUC reduce surface temperature by boosting evapotranspiration. As a result, upwelling longwave is reduced (net LW increased) and LUC-induced evaporative cooling is damped. That said, the amplitude of ΔLW is weak compared with ΔLH and ΔSH . Despite its strong correlation with heat extremes, longwave radiation only plays the second-order role of damping the first-order effect of evaporative cooling.

Albedo is often the main property of interest when considering the biophysical effects of forestation, since trees tend to be darker than grasses (Hasler 2024). During winter and spring, albedo exerts a strong influence on temperature as snow covers forested and deforested regions (figure SI-T2). However, in the present case of summertime and with LUC dominated by broadleaf forestation of grasslands, albedo is not so important. In our model, broadleaf trees have a marginally smaller visible albedo than grasses ($\alpha = 0.05$ vs 0.06 ; see table SI-LC1), hence LUC induce only weak changes in shortwave radiation. In fact, the correlation between LUC-induced, hot-day ΔSW and ΔTX is negative ($R = -0.32$), meaning that excess shortwave radiation tends to be co-located with *reduced* heat extremes. This is the opposite of what would be expected in a situation of shortwave-driven warming.

In summary, the main effect of LUC on the hot-day surface energy balance is to shift the partition of turbulent fluxes away from sensible heat and towards latent heat fluxes. Incident solar energy that would otherwise warm the surface and the air above is instead utilized to evaporate water, hence



cooling results. Planck's feedback acts to reduce this cooling effect, but its magnitude is relatively weak. Albedo changes are insufficient to drive appreciable shortwave-driven warming.

4. Blue in green: changes in water fluxes

The concepts of blue and green water offer a compelling way to think about changes in the water cycle (Falkenmark 1995, Falkenmark and Rockström 2006, Mastrotheodoros 2020, Stewart-Koster 2024). Blue water comprises streams, lakes, reservoirs and aquifers. It is the surface and groundwater available to human use. Green water, on the other hand, is plant-available water. It represents the component of precipitation that does not run off and is instead absorbed by the soil and used by plants. In section 3, we found that the heat relief provided by forestation requires an increase in green water fluxes, or latent heat fluxes. This begs the question: where does this supplementary water come from? Do LUC enhance precipitation, or reduce blue water fluxes? To properly answer these questions, we analyse how LUC affect the annual and seasonal water flux budgets.

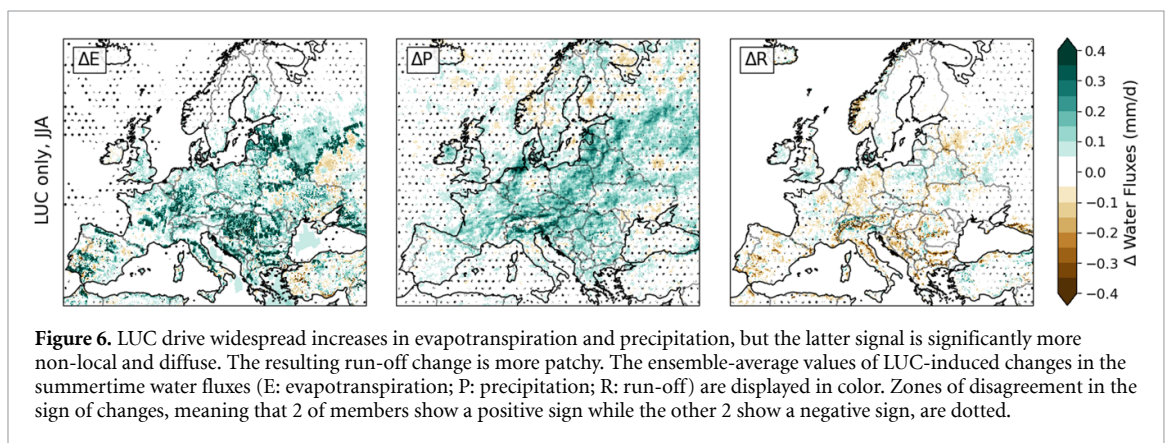
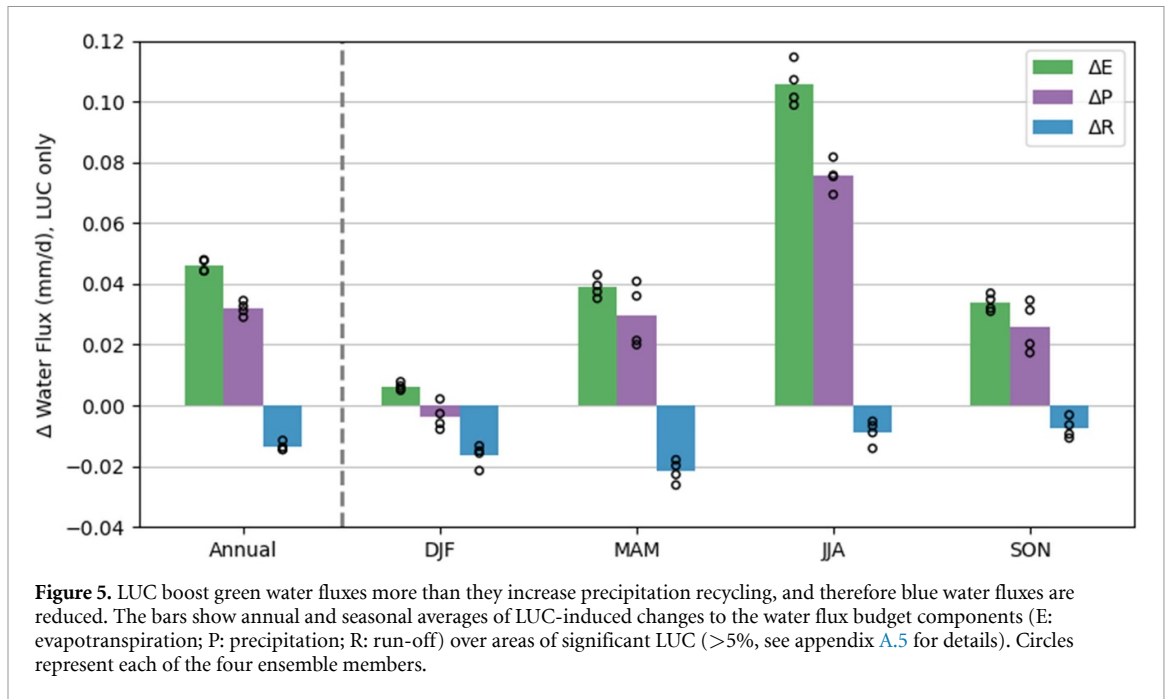
4.1. Forestation turns blue water green

We have seen in previous sections that LUC increase evapotranspiration (E) during hot summer days. This remains true for seasonal averages all year round (green bars in figure 5): LUC boost green water fluxes by 0.046 mm d^{-1} on average over the year. This rather small number conceals important seasonal variability. Since vegetation is most active during the warmer months of the year, there is a strong seasonal cycle in ΔE . While LUC have nearly no effect during winter, they increase E by more than 0.1 mm d^{-1} on average during the summer. These seasonal averages have weak inter-member variability (see limited spread in the black dots depicting individual member values, figure 5). The highly structured spatial patterns of ΔE (figure 6) and their resemblance to LUC patterns suggest that the evaporative response

is dominated by local changes in the biophysical properties of the surface, with secondary dependence on climate variability and local/regional atmospheric feedbacks.

LUC also increase annual precipitation by 0.032 mm d^{-1} on average (purple bars in figure 5). The seasonal cycle of ΔP resembles that of ΔE although with weaker amplitude, ranging from negligible wintertime change to peak boost in summer at about 0.07 mm d^{-1} . Since LUC-induced differences are calculated between couples of simulations with identical atmospheric and oceanic conditions at the boundaries, ΔP can be interpreted as regional precipitation recycling (Eltahir and Bras 1996, Tuinenburg *et al* 2020). Prevailing winds being westerly, there is little to no agreement in the sign of ΔP upwind (west) of the land mass (figure 6). The most robust component of the signal is the widespread increase of ΔP over continental Europe during the summer. Compared with ΔE , the ΔP signal is much smoother, hinting at the more non-local character of precipitation recycling (Meier *et al* 2021, te Wierik *et al* 2021). The spatial variability of continental summertime ΔP is relatively robust across members, although there is more disagreement than for ΔE in some regions. During the other seasons, there is little agreement in the signal (figure SI-WF1). Nevertheless, the spatiotemporal average shows a robust increase in annual precipitation.

Annual LUC-induced ΔE is greater than ΔP by about 0.014 mm d^{-1} . Annual run-off (R), or the blue water flux, is thus reduced by a comparable amount (blue bars in figure 5). In our model, R is the sum of surface and deep run-off (figure SI-WF2). Surface run-off has a relatively weak contribution to ΔR , except during winter and spring as snow-related dynamics come into effect (figure SI-SN). Total ΔR is mostly driven by changes in deep run-off, which have a less pronounced seasonal cycle. The seasonal cycle of ΔR is out of phase with that of ΔE and ΔP : peak ΔR occurs in spring, with most modest values during summer and fall.

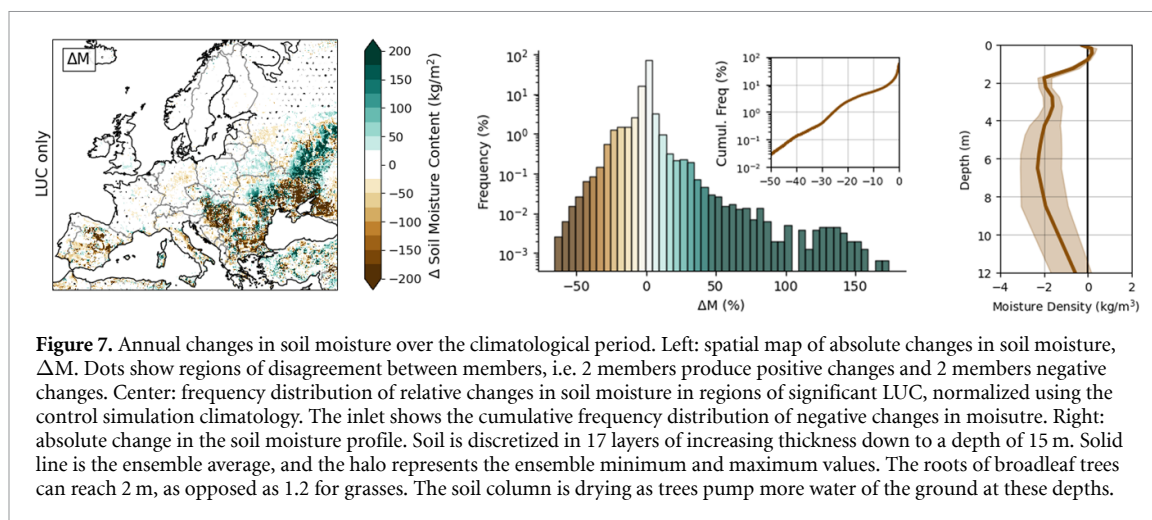


4.2. Impact on soil moisture

The climatology of soil moisture, M , is significantly influenced by forestation (figure 7). While the northwest portion of Europe experiences only superficial changes, the south and southeast of the continent show both areas of strong replenishment and drying, especially north of the Black Sea and in the Hungarian plains. LUC contribute to the drying of these regions because LUC-induced precipitation recycling does not match the blue-to-green water flux shift. Furthermore, since these regions have relatively dry soils in the first place, the relative changes in soil moisture can be drastic. In particular, about 1% of the significant-LUC grid cells undergo a drying exceeding 25%, and 0.1% dry by 40% or more (figure 7, middle panel).

Inspection of the vertical profile of spatially-averaged ΔM , depicted in the right panel of figure 7, is also instructive. While LUC cause no net moisture change in the first top meter of soil, a significant drop

in moisture becomes apparent below 1 m. The drop of moisture below 1 m is compelling evidence that forestation modulates the water budget by pumping of water deeper in the soil than grasses and crops would. In our model, broadleaf trees have 2 m deep root whereas grasses, which are the main land cover replaced by forestation, have 1.2 m deep root (table SI-LC1). With broadleaf-tree forestation, soil moisture between 1.2 and 2 m becomes available for pumping. As a result, forestation-induced evapotranspiration drains additional moisture between 1.2 and 2 m. This slows percolation of soil moisture to deeper layers and hence reduced deep drainage (negative ΔR). The LUC-induced moisture profile has an about 2 kg m^{-3} moisture deficit extending from about 2 m down to almost the whole soil column. In summary, moisture profiles reveal a clear signature of root deepening with forestation, and enhanced evapotranspiration by broadleaf trees is associated with reduced deep soil moisture and drainage.



5. Discussion

5.1. The blue-green trade-off

In this paper, we used an ensemble of regional climate simulations to weave together a narrative of the effects of large-scale forestation in Europe under SSP1-2.6. In essence, we found that forestation brings heat relief by turning blue water green, compromising water availability in some already-dry regions. Ambitious forestation plans thus introduce a thorny trade-off between heat mitigation and water availability (Jackson *et al* 2005). On the one hand, large-scale broadleaf forestation would boost carbon sequestration and green water fluxes, both mitigating the negative impact of extreme summer heat. On the other hand, more green water means less blue water in the soil, streams, reservoirs and aquifers essential to support human life and other ecosystem services. To complicate matters, forestation has non-local effects on precipitation. One region's decision to plant trees for heat relief may affect another region's hydrology.

5.2. Comparison with the recent literature

How well does this narrative hold against other lines of observational and modeling evidence in the literature? Over large parts of continental Europe, we find that LUC trump GHG, resulting in milder heat waves at the end of the century compared with today (figure 3). Using four ESMs, Hirsch *et al* (2018) also found LUC to contribute significantly to the heat extremes in low-emission scenarios, although typically less so than other forcings combined and with more variability in the sign of change. There is nevertheless considerable observational evidence that the presence (absence) of forests is associated with reduced (increased) heat extremes (Li *et al* 2015, Alkama and Cescatti 2016). Lejeune *et al* (2018) used an observationally-constrained climate simulation ensemble to show that historical deforestation increased the intensity of hot days in northern mid-latitudes. Similarly, satellite observations of the recent vegetation greening in China were associated with

reduced mean and extreme temperatures (Cao *et al* 2023). There is further satellite-based (Schwaab *et al* 2020) and modeling-based (Breil *et al* 2023) evidence that broadleaf trees provide more heat relief than needleleaf trees, as was found here.

To identify the mechanisms responsible for the heat relief, we analyzed how LUC alter the surface energy balance (section 3.2). Consistent with in-situ and remote sensing observations (Bright *et al* 2017), we find that LUC primarily affect non-radiative processes (figure 4). Duveiller *et al* (2018) estimated the effects of different various LUC on the surface energy balance using remote sensing observations. Their deciduous broadleaf forest to grasses transition shows the same sign of change as our analysis for all energy fluxes, except for their weak sensible heat signal. Li *et al* (2015) also demonstrate that during summer, the effects of enhanced evapotranspiration outweigh those of albedo, leading to lower daily temperatures over northern mid-latitude forests compared to open lands. Likewise, Zeng *et al* (2017) identify evapotranspiration as the main agent driving biophysical cooling associated with Earth's greening.

In section 4, we explored the implications of large-scale forestation on the water cycle. In our simulation ensemble, forestation boosts both evapotranspiration and precipitation (figures 5 and 6). This aligns with observational studies showing that LUC in Europe over the past decades—mainly forestation of rain-fed agricultural lands—have resulted in increased evapotranspiration (Teuling *et al* 2019) and precipitation (Meier *et al* 2021). Similar changes have been observed following afforestation of the Chinese Loess Plateau (Tian *et al* 2022). Our resulting runoff signal is weaker and patchy, but negative on average over regions of significant LUC, consistent with the well-known drying of streams typically following forestation (Bosch and Hewlett 1982, Jackson *et al* 2005). We also find that LUC-induced changes in the water cycle can cause significant drying of the soil column in already-dry regions (Ge *et al* 2023; see figure 7). Hoek van Dijke *et al* (2022) estimated that

global tree restoration could decrease water availability by up to 38% in some regions, which is on par with our findings (figure 7).

5.3. Limitations

While this study provides a self-consistent illustration of the linkage between forestation, climate and hydrology, a myriad of limitations hinders its direct use for policy decisions. First and foremost, our study captures a small fraction of total uncertainty. We explored LUC under SSP1-2.6, which, although a standard scenario in climate modeling (O'Neill 2016), represents just one plausible outcome among countless possible futures. It would be surprising, in fact, if heat extremes were also alleviated in less optimistic scenarios, which include both more emissions and less forestation. Next, using a four-member ensemble of MPI-ESM simulations is a good start for accounting for this ESM's internal variability, but it is definitely insufficient. We chose this ESM in particular because of its plausible 3 °C climate sensitivity, but a single ESM is cannot capture the breadth of plausible outcomes, even within a specific scenario. A few multi-ESM comparison studies have been conducted specifically on the subject of LUC (notably Lawrence 2016, Hirsch 2018, Lejeune *et al* 2018, Seneviratne 2018), but high intermodel variability makes an in-depth exploration of mechanisms much more challenging.

Furthermore, the global climate data was down-scaled using a single RCM. There is also considerable variability in the response to LUC among RCM-LSM (Davin 2020, Asselin *et al* 2022). Fortunately, the ongoing second phase of CORDEX Flagship Pilot Project LUCAS is expected to provide a more detailed analysis of variability to be expected across RCMs and land surface model using the same land cover maps. Finally, the land surface model used here, CLASS, remains a relatively crude parametric representation of vegetation, which in reality behaves in a highly complex manner. To this we must add the high uncertainty related to the creation of land cover maps, especially their projection in the future (Reinhart *et al* 2022b, Hoffmann *et al* 2023).

6. Conclusion

Meeting the stringent carbon budget set forth by the Paris Agreement would likely imply substantial changes in land-use. This paper explores the SSP1-2.6 scenario, a possible future with significant emissions reductions and ambitious forestation efforts. To achieve this, we employ a RCM that fully couples land and atmospheric processes at high spatial resolution and enables a clear separation of the effects of LUC and GHG on regional climate. The main contribution of this study is to illustrate the mechanisms linking LUC, heat extremes, and water availability within a single self-consistent framework, effectively bridging

key but typically isolated results from the climate and hydrology communities. We now conclude with a brief summary of the main results highlighted by our regional climate simulation ensemble:

- Forestation mitigates summer heat extremes more than GHG exacerbate them over large swath of continental Europe. End-of-century heat waves may be *milder* than today in some regions thanks to forestation (figure 3).
- This heat relief is attributed to a rerouting of energy flows, namely a shift from sensible to latent heat fluxes (figure 4). Energy which would otherwise warm the surface and the air above is utilized to evaporate water. Net cooling results.
- At continental scale, forestation induces regional precipitation recycling, but not enough to match the boost of evapotranspiration (green water flux). Run-off (blue water flux) is reduced as a result (figure 5). Put simply, forestation turns blue water green.
- Enhanced evapotranspiration is mainly driven by local changes in the biophysical properties of the surface. The boost of precipitation has a comparatively smooth and non-local character. The resulting run-off signal has high spatial variability (figure 6).
- Regions in the southeast of Europe undergo significant changes in soil moisture. Some already-dry regions experience significant drying (figure 7).

Data availability statement

The data that support the findings of this study are available upon reasonable request from the authors.

Acknowledgments

Computations were carried on the SuperMUC-NG supercomputer at the Leibniz Supercomputing Centre (LRZ) of the Bavarian Academy of Sciences and Humanities.

Appendix

A.1. Isolating LUC and GHG effects

To estimate the effects of greenhouse gases (GHGs) and land-use changes (LUC) on a variable of interest, we compute how this variable changes between simulation ensembles with different configurations, i.e. land cover and GHG concentration (figure 1). For instance, the effect of GHGs on temperature (T) is given by

$$\Delta_{\text{GHG}}T = T_{G_p L_p} - T_{G_p}, \quad (1)$$

where the absence of a superscript on G signals that we summed over the $N = 4$ members to obtain the

ensemble average, for instance:

$$T_{G_p L_p} = \frac{1}{N} \sum_{X=1}^N T_{G_p^X L_p}. \quad (2)$$

Similarly, the temperature change due to LUC reads as

$$\Delta_{\text{LUC}} T = T_{G_f L_f} - T_{G_p L_p}. \quad (3)$$

Finally, to obtain the combined influence of LUC and GHGs, we compute:

$$\Delta_{\text{GHG+LUC}} T = T_{G_f L_f} - T_{G_p L_p}. \quad (4)$$

A.2. Summer heat extremes

This paper focuses on summer heat extremes, which we define using the 95th percentile of daily maximum temperature (TX95). To obtain this quantity, we sort the maximum daily temperatures (TX) of all days of June, July and August (JJA) from all four members, and extract the 95th percentile. This is done independently for each of the three model configurations, i.e. land cover and GHG concentration, such that each configuration is associated with a unique TX95. The effects of GHG and LUC on heat extremes can then be calculated by replacing T with TX95 in equations (1) and (3), the result of which is displayed in figure 3.

A.3. Population exposed to milder heat extremes

To provide a rough estimate of the population exposed to milder heat extremes, we use contemporary population data from the version 3.3 of the History Database of the Global Environment (HYDE; Klein Goldewijk *et al* 2017). The heat extreme maps of figure 2 are re-gridded to the 2023 population map using bilinear interpolation (figure SI-T1). For this analysis, only European countries are considered, excluding Russia, Turkey, Georgia, Azerbaijan, and Cyprus. The total 2023 population included in this domain is about 575 million, of which 277 million (i.e. 48%, or about half) would experience milder heat extremes in simulations with both emissions and LUC. When only the effects of emissions are included, this number drops to 8 million or about 1%.

A.4. Hot days

The analysis of section 3.2 focuses on hot summer days. We define hot days as summer (JJA) days with a maximum daily temperature (TX) exceeding its 95th percentile (TX95) for a given configuration. Therefore, once TX95 is known, a list of hot days can be generated:

$$D^{\text{hot}} \equiv \{d_1, d_2, \dots, d_M\} \quad (5)$$

where d_i 's are all days such that

$$\text{TX}(d_i) > \text{TX95} \quad (6)$$

Again, this is done independently for each of the three model configurations. As a result, each configuration is associated with the same number of hot days, M .

Once the hot-day list is generated, the hot-day average of any variable of interest can be obtained. For instance,

$$\text{LH}^{\text{hot}} = \frac{1}{M} \sum_{t \in D^{\text{hot}}} \text{LH}(t), \quad (7)$$

where $\text{LH}(t)$ is the daily average value of latent heat fluxes for a given configuration. By taking the difference between hot-day averages with and without LUC (i.e. following equation (3)), one can estimate the effect of LUC on hot-day latent heat fluxes, $\Delta_{\text{LUC}} \text{LH}^{\text{hot}}$ (or simply ΔLH in the text of section 3.2), as was done in figure 4.

A.5. Spatial integration and areas of significant LUC

In this paper, there are several calculations involving horizontal spatial integration (or averaging): the correlations between LUC, climatic and hydrological variables (section 3), the water fluxes budget (section 4.1) and the vertical profile of soil moisture (section 4.2). To emphasize the effects of LUC, all spatial integrals are calculated over areas of significant LUC only. We set the significance threshold to 5%, meaning that a grid point is considered to undergo significant LUC if any of the aggregated land cover categories—broadleaf trees, needleleaf trees, crops, urban, shrubs or grasses—is associated with a change superior to 5% of the tile area.

ORCID iDs

Olivier Asselin  <https://orcid.org/0000-0003-3621-2737>

Martin Leduc  <https://orcid.org/0000-0002-1596-3788>

Dominique Paquin  <https://orcid.org/0000-0002-1353-930X>

Diana Rechid  <https://orcid.org/0000-0002-6035-2935>

Ralf Ludwig  <https://orcid.org/0000-0002-4225-4098>

References

- Alkama R and Cescatti A 2016 Biophysical climate impacts of recent changes in global forest cover *Science* **351** 600–4
- Asselin O, Leduc M, Paquin D, Di Luca A, Winger K, Bukovsky M, Music B and Giguère M 2022 On the intercontinental transferability of regional climate model response to severe forestation *Climate* **10** 138
- Betts R A 2000 Offset of the potential carbon sink from boreal forestation by decreases in surface albedo *Nature* **408** 187–90
- Bonan G B 2001 Observational evidence for reduction of daily maximum temperature by croplands in the Midwest United States *J. Clim.* **14** 2430–42

- Bosch J M and Hewlett J 1982 A review of catchment experiments to determine the effect of vegetation changes on water yield and evapotranspiration *J. Hydrol.* **55** 3–23
- Breil M, Weber A and Pinto J G 2023 The potential of an increased deciduous forest fraction to mitigate the effects of heat extremes in Europe *Biogeosciences* **20** 2237–50
- Bright R M, Davin E, O'Halloran T, Pongratz J, Zhao K and Cescatti A 2017 Local temperature response to land cover and management change driven by non-radiative processes *Nat. Clim. Change* **7** 296–302
- Cao Y, Guo W, Ge J, Liu Y, Chen C, Luo X and Yang L 2023 Greening vegetation cools mean and extreme near-surface air temperature in China *Environ. Res. Lett.* **19** 014040
- Chen L and Dirmeyer P A 2019 The relative importance among anthropogenic forcings of land use/land cover change in affecting temperature extremes *Clim. Dyn.* **52** 2269–85
- Davin E L et al 2020 Biogeophysical impacts of forestation in Europe: first results from the LUCAS (Land Use and Climate Across Scales) regional climate model intercomparison *Earth Syst. Dyn.* **11** 183–200
- Doelman J C et al 2018 Exploring SSP land-use dynamics using the IMAGE model: regional and gridded scenarios of land-use change and land-based climate change mitigation *Glob. Environ. Change* **48** 119–35
- Duveiller G, Hooker J and Cescatti A 2018 The mark of vegetation change on Earth's surface energy balance *Nat. Commun.* **9** 1–12
- Ellison D et al 2017 Trees, forests and water: cool insights for a hot world *Glob. Environ. Change* **43** 51–61
- Ellison D, Futter M N and Bishop K 2012 On the forest cover–water yield debate: from demand-to supply-side thinking *Glob. Change Biol.* **18** 806–20
- Eltahir E A and Bras R L 1996 Precipitation recycling *Rev. Geophys.* **34** 367–78
- Engel F, Hoek van Dijke A J, Roebroek C T and Benedict I 2024 Can large-scale tree cover change negate climate change impacts on future water availability? *EGU sphere* **2024** 1–32
- Falkenmark M 1995 Coping with water scarcity under rapid population growth *Conf. of SADC Ministers, Pretoria* vol 23 p 24
- Falkenmark M and Rockström J 2006 The new blue and green water paradigm: breaking new ground for water resources planning and management *J. Water Resour. Plan. Manag.* **132** 129–32
- Ge F, Xu M, Li B, Gong C and Zhang J 2023 Afforestation reduced the deep profile soil water sustainability on the semiarid Loess Plateau *Forest Ecol. Manage.* **544** 121240
- Harper A B et al 2018 Land-use emissions play a critical role in land-based mitigation for Paris climate targets *Nat. Commun.* **9** 2938
- Hasler N et al 2024 Accounting for albedo change to identify climate-positive tree cover restoration *Nat. Commun.* **15** 2275
- Hirsch A L et al 2018 Biogeophysical impacts of land-use change on climate extremes in low-emission scenarios: results from HAPPI-Land *Earth's Future* **6** 396–409
- Hoek van Dijke A J, Herold M, Mallick K, Benedict I, Machwitz M, Schlerf M, Pranindita A, Theeuwes J J, Bastin J-F and Teuling A J 2022 Shifts in regional water availability due to global tree restoration *Nat. Geosci.* **15** 363–8
- Hoffmann P, Reinhart V and Rechid D 2022 LUCAS LUC future land use and land cover change dataset for Europe (Version 1.1) (available at: https://doi.org/10.26050/WDCC/LUC_future_EU_v1.1)
- Hoffmann P, Reinhart V, Rechid D, de Noblet-Ducoudré N, Davin E L, Asmus C, Bechtel B, Böhner J, Katragkou E and Luyssaert S 2023 High-resolution land use and land cover dataset for regional climate modelling: historical and future changes in Europe *Earth Syst. Sci. Data* **15** 3819–52
- Huang B, Hu X, Fuglstad G-A, Zhou X, Zhao W and Cherubini F 2020 Predominant regional biophysical cooling from recent land cover changes in Europe *Nat. Commun.* **11** 1066
- Hurt G C et al 2020 Harmonization of global land use change and management for the period 850–2100 (LUH2) for CMIP6 *Geosci. Model Dev.* **13** 5425–64
- Jackson R B, Jobbágy E G, Avissar R, Roy S B, Barrett D J, Cook C W, Farley K A, Le Maitre D C, McCarl B A and Murray B C 2005 Trading water for carbon with biological carbon sequestration *Science* **310** 1944–7
- Klein Goldewijk K, Beusen A, Doelman J and Stehfest E 2017 Anthropogenic land use estimates for the Holocene–HYDE 3.2 *Earth Syst. Sci. Data* **9** 927–53
- Lawrence D M et al 2016 The Land Use Model Intercomparison Project (LUMIP) contribution to CMIP6: rationale and experimental design *Geosci. Model Dev.* **9** 2973–98
- Lee X et al 2011 Observed increase in local cooling effect of deforestation at higher latitudes *Nature* **479** 384–7
- Lejeune Q, Davin E L, Gudmundsson L, Winckler J and Seneviratne S I 2018 Historical deforestation locally increased the intensity of hot days in northern mid-latitudes *Nat. Clim. Change* **8** 386–90
- Li Y, Zhao M, Motesharrei S, Mu Q, Kalnay E and Li S 2015 Local cooling and warming effects of forests based on satellite observations *Nat. Commun.* **6** 6603
- Martynov A, Laprise R, Sushama L, Winger K, Šeparović L and Dugas B 2013 Reanalysis-driven climate simulation over CORDEX North America domain using the Canadian Regional Climate Model, version 5: model performance evaluation *Clim. Dyn.* **41** 2973–3005
- Mastrotheodoros T et al 2020 More green and less blue water in the Alps during warmer summers *Nat. Clim. Change* **10** 155–61
- Matte D, Laprise R, Thériault J M and Lucas-Picher P 2017 Spatial spin-up of fine scales in a regional climate model simulation driven by low-resolution boundary conditions *Clim. Dyn.* **49** 563–74
- Mauritsen T et al 2019 Developments in the MPI-M Earth System Model version 1.2 (MPI-ESM1.2) and its response to increasing CO₂ *J. Adv. Model. Earth Syst.* **11** 998–1038
- Meier R, Schwaab J, Seneviratne S I, Sprenger M, Lewis E and Davin E L 2021 Empirical estimate of forestation-induced precipitation changes in Europe *Nat. Geosci.* **14** 473–8
- O'Neill B C et al 2016 The scenario model intercomparison project (ScenarioMIP) for CMIP6 *Geosci. Model Dev.* **9** 3461–82
- Perugini L, Caporaso L, Marconi S, Cescatti A, Quesada B, de Noblet-Ducoudre N, House J I and Arneft A 2017 Biophysical effects on temperature and precipitation due to land cover change *Environ. Res. Lett.* **12** 053002
- Pongratz J, Schwingshackl C, Bultan S, Obermeier W, Havermann F and Guo S 2021 Land use effects on climate: current state, recent progress and emerging topics *Current Clim. Change Rep.* **7** 99–120
- Popp A et al 2017 Land-use futures in the shared socio-economic pathways *Glob. Environ. Change* **42** 331–45
- Reinhart V, Hoffmann P and Rechid D 2022a LANDMATE PFT land cover dataset for Europe 1992–2015 (Version 1.1) (available at: https://doi.org/10.26050/WDCC/LM_PFT_EUR_v1.1)
- Reinhart V, Hoffmann P, Rechid D, Böhner J and Bechtel B 2022b High-resolution land use and land cover dataset for regional climate modelling: a plant functional type map for Europe 2015 *Earth Syst. Sci. Data* **14** 1735–94
- Roe S et al 2019 Contribution of the land sector to a 1.5 C world *Nat. Clim. Change* **9** 817–28
- Schwaab J, Davin E L, Bebi P, Duguay-Tetzlaff A, Waser L T, Haeni M and Meier R 2020 Increasing the broad-leaved tree fraction in European forests mitigates hot temperature extremes *Sci. Rep.* **10** 14153
- Seneviratne S I et al 2018 Climate extremes, land–climate feedbacks and land-use forcing at 1.5 C *Phil. Trans. R. Soc. A* **376** 20160450
- Šeparović L, Alexandru A, Laprise R, Martynov A, Sushama L, Winger K, Tete K and Valin M 2013 Present climate and

- climate change over North America as simulated by the fifth-generation Canadian regional climate model *Clim. Dyn.* **41** 3167–201
- Stewart-Koster B *et al* 2024 Living within the safe and just Earth system boundaries for blue water *Nat. Sustain.* **7** 53–63
- te Wierik S A, Cammeraat E L, Gupta J and Artzy-Randrup Y A 2021 Reviewing the impact of land use and land-use change on moisture recycling and precipitation patterns *Water Resour. Res.* **57** e2020WR029234
- Tebaldi C *et al* 2020 Climate model projections from the scenario model intercomparison project (ScenarioMIP) of CMIP6 *Earth Syst. Dyn. Discuss.* **2020** 1–50
- Teuling A J, De Badts E A, Jansen F A, Fuchs R, Buitink J, Hoek van Dijke A J and Sterling S M 2019 Climate change, reforestation/afforestation and urbanization impacts on evapotranspiration and streamflow in Europe *Hydrol. Earth Syst. Sci.* **23** 3631–52
- Tian L, Zhang B, Chen S, Wang X, Ma X and Pan B 2022 Large-scale afforestation enhances precipitation by intensifying the atmospheric water cycle over the Chinese Loess Plateau *J. Geophys. Res. Atmos.* **127** e2022JD036738
- Tuinenburg O A, Theeuwes J J and Staal A 2020 High-resolution global atmospheric moisture connections from evaporation to precipitation *Earth Syst. Sci. Data* **12** 3177–88
- Verseghy D L 1991 CLASS—a Canadian land surface scheme for GCMs. I soil model *Int. J. Clim.* **11** 111–33
- Verseghy D, McFarlane N and Lazare M 1993 CLASS—a Canadian land surface scheme for GCMs, II. Vegetation model and coupled runs *Int. J. Climatol.* **13** 347–70
- Zeng Z *et al* 2017 Climate mitigation from vegetation biophysical feedbacks during the past three decades *Nat. Clim. Change* **7** 432–6